MICROVASCULAR RESEARCH 50, 397–416 (1995)

Neutrophil Migration through Preexisting Holes in the Basal Laminae of Alveolar Capillaries and Epithelium during Streptococcal Pneumonia

DAVID C. WALKER, ALI R. BEHZAD, AND FANNY CHU

University of British Columbia, Pulmonary Research Laboratory, St. Paul's Hospital, Vancouver, British Columbia, Canada

Received April 4, 1995

The purpose of this study was to determine whether or not there are preexisting holes in the endothelial and epithelial basal laminae of alveolar walls and to determine the path taken by neutrophils as they migrate from the capillaries to the airspace of the alveoli during inflammation. Using transmission electron microscopy and serial thin sections of normal rabbit and mouse lung, we have demonstrated the presence of slit-like holes in the capillary basal laminae and round holes in the basal laminae of type 2 pneumocytes. The slits in the capillary basal laminae were observed at the intersection of the thick and thin walls where endothelium, pericytes, and fibroblasts make close contact. The round holes in the type 2 cell basal laminae were observed at sites of close contact with fibroblasts. Neutrophils were observed to migrate through these slits and holes during streptococcal pneumonia in rabbit lungs. We conclude that during inflammation in the lung, migrating neutrophils displace pericytes and fibroblasts from the slits in the capillary basal lamina and then crawl through these slits into the alveolar interstitium. We postulate that neutrophils find their way to type 2 pneumocytes by following interstitial fibroblasts. We believe that neutrophils displace fibroblasts from their close contacts with the type 2 cells and then crawl through the holes in the basal lamina into the basal lateral space of the type 2 cells. From there, neutrophils migrate into the alveolar airspace.

INTRODUCTION

Neutrophils emigrate out of lung capillaries during an inflammatory reaction (Loosli and Baker, 1962; Meyrick and Brigham, 1983; Shaw, 1980; Lien *et al.*, 1991; Walker *et al.*, 1991) and emerge from the alveolar walls into the airspace between the type 2 pneumocytes and their neighboring type 1 pneumocytes (Damiano *et al.*, 1980). These observations suggest that migrating neutrophils must make their way from the capillaries to a type 2 pneumocyte and then into the airspace.

The capillary basal lamina that is next to the airspace is fused with the alveolar epithelial basal lamina (Low, 1961; Gil and Weibel, 1969; Ryan, 1969; Sannes, 1984; Cottrell *et al.*, 1967). This region of fused basal laminae is the thin wall of the capillary. On the opposite, or thick side of the capillary, the interstitial space is larger and contains a variety of extracellular matrix elements and cells. These matrix elements include fibrillar collagen, elastin, reticulin, and proteoglycans (Wang and Ying, 1977; Kefalides *et al.*, 1979; Zibrak *et al.*, 1981; Martinez-Hernandez *et al.*, 1983). The basal lamina which lies underneath the alveolar epithelium (Low, 1961; Gil and

0026-2862/95 $12.00

Weibel, 1969; Ryan, 1969) is richer in proteoglycans under the type 1 pneumocytes than it is under the type 2 pneumocytes (Sannes, 1984). The majority of cells found in the interstitium of the alveolar wall are fibroblasts of at least two morphologically distinct types (Kaplan *et al.*, 1985; Brody and Nancy, 1983; Penny *et al.*, 1992; Phipps, 1992). A smaller number of pericyte cell bodies with their basal lamina are also found in the interstitium (Sims and Westfall, 1983).

Following diapedesis across the endothelium the neutrophils cross the endothelial basal lamina and then enter the interstitium. They migrate through the interstitium to the nearest type 2 pneumocyte, make their way through the epithelial basal lamina, and diapede between the type 2 and type 1 pneumocytes into the airspace (Damiano *et al.*, 1980). The purpose of this study was to determine whether or not there are preexisting holes in endothelial and epithelial basal laminae that might facilitate the migration of neutrophils and to determine how neutrophils migrate across endothelial and epithelial basal laminae during streptococcal pneumonia.

MATERIALS AND METHODS

Animals. Three healthy female New Zealand White rabbits that weighed 2–3.5 kg and three healthy 20-g female Balb C mice were used as control animals. The observations of migrating neutrophils included in this study came from an additional three female New Zealand White rabbits of the same weight range as the controls. However, they each had a streptococcal pneumonia of 2-hr duration at the time of sacrifice.

Protocol. The rabbits were anesthetized with ketamine hydrochloride (25–40 mg/kg) and acepromazine maleate (2–3 mg/kg) by intramuscular injection. The mice were anesthetized by intraperitoneal injection of 0.1 ml of urethane (50% in sterile saline). Pneumonia was produced in three of the rabbits by instillation of 0.6 ml of a solution of *Streptococcus pneumoniae* (5×10^8 cells) and colloidal carbon (0.05 ml of India ink in the 0.6 ml of instillate) in sterile saline following a protocol described by Doerschuk *et al.* (1990).

Sacrifice/fixation. The rabbits were sacrificed by perfusion fixation (Walker *et al.*, 1994) either immediately after anesthesia or at 2 hr after instillation of *S. pneumoniae.* Briefly, catheters (22G, Jelco iv catheters, Tampa, FL) were placed in the internal left jugular vein and the right common carotid artery. The abdominal aorta and the vena cava were occluded by hemostat through a small abdominal incision just below the diaphragm to avoid perfusion of the abdominal organs and hind limbs. The left jugular vein catheter was connected to a double reservoir by a three-way valve to permit sequential perfusion with heparinized Krebs buffer (pH 7.4) followed by 2.5% glutaraldehyde in cacodylate buffer (0.1 *M* at pH 7.4) containing 0.01% toluidine blue dye. The right common carotid catheter was used as a drain. Colloidal carbon marked the lung region containing bacterial instillate (Doerschuk *et al.*, 1990) and the toluidine blue marked the areas that were fixed (Walker *et al.*, 1994).

In the mice, the left internal jugular vein was catheterized using a dissecting microscope and then the abdominal aorta was severed as a drain. Thus, the mouse lungs were fixed *in situ,* without entering the thorax, by perfusing glutaraldehyde through the left internal jugular vein cannula and draining fluids from the abdominal aorta.

For both the rabbits and the mice, the chest cavity was opened 15 min after perfusion fixation and the lungs were removed. The lungs were then stored in 2.5% glutaraldehyde overnight at 4°C.

Tissue sampling of rabbit and mouse lungs. For each animal a 1.5-mm slice was cut from the bottom right and left lower lobes of the lungs. Using a dissecting microscope, a 2-mm wide strip was cut from the middle of each of the two slices. These strips were then cut into 1-mm cubes. Cubes that included central airways or large vessels were discarded. A 1.5-mm vertical slice was cut from the middle of either the right or left lower lobe in a coronal plane. Another 2-mm strip was cut across this slice and then cut into 1-mm cubes containing only lung parenchyma. For each animal the 1-mm cubes from the two horizontal and one vertical slices were mixed. All of the cubes were then washed three times with 0.1 *M* cacodylate buffer at pH 7.4. After the washes, the tissues were incubated in 1% tannic acid for 1 hr prior to postfixation in a solution of 1% tannic acid and 1% osmium tetroxide in 0.1 *M* cacodylate buffer at pH 7.4 (Sanders, 1983). After three washes with distilled water, the tissues were dehydrated through ethanol, transferred to propylene oxide, and infiltrated with Epon 812.

Six blocks of lung were randomly picked from each animal and thin sectioned on a Reichert ultramicrotome. Uranyl acetate and Sato's (1968) lead-stained sections were viewed on a Philips 400 TEM. For each block the first five cross-sectioned alveolar capillaries observed (width:height ratio = 1) were photographed at 3000 to 6000× so as to include the whole capillary (Fig. 1a). Two more micrographs of each capillary were taken at 12,500 to 16,000× to cover the two intersections of the thick and thin walls of the capillaries (Fig. 1b). Therefore, sampling included the examination of 30 capillaries from each animal. The capillary profiles were divided into three regions; the thin wall, the thick wall, and the intersection of the thick and thin wall (Fig. 1a). The locations of endothelial tight junctions, pericytes, fibroblasts, and basal lamina holes were tabulated by region (thick wall, thin wall, or intersection) for each capillary profile.

Serial sectioning, rabbit capillaries. Seven blocks (minimum two/rabbit) were randomly selected for serial sectioning. A 0.5-μm section was cut from each block, stained with toluidine blue, and examined for the presence of a cross-sectioned capillary. The block was then retrimmed around the selected cross-sectioned capillary and 20 80-nm-thick serial sections were cut. The thin sections were picked up on Formvar-coated slot grids, 5 sections per grid. The selected capillary was then photographed with the Philips 400 in each of the 20 serial sections. The micrographs of the capillary in all 20 sections from each of the serial-sectioned capillaries were examined for the presence of contacts among the endothelial cells, pericytes, and pulmonary fibroblasts. The sizes of these contacts were estimated by measuring their widths and lengths. Their widths were determined by measuring the size of the contact area on each section. Their lengths were determined by counting the number of serial sections in which they occurred. For one capillary we collected 19 serial sections and reconstructed it by making tracings on sheets of cardboard the same thickness as the sections at 16,200× in order to illustrate contact size and locations.

Serial sectioning, rabbit type 2 pneumocytes. Unused blocks from control lung parenchyma were trimmed so that the leading and trailing edges were not less than 0.3 mm long. These blocks were then coated with one drop of an adhesive solution prepared from cellophane tape according to the method of Marko *et al.* (1988). This adhesive held the ribbons of serial sections together so that it was possible to cut and collect as many 0.2-μm serial sections on Formvar-coated grids as desired without interruption. All sections were stained in 2% aqueous uranyl acetate at 60°C for 10

min and then stained with Reynold's lead citrate for 10 min at 25°C. All sections were viewed and photographed with a Philips 400 TEM. For this study we cut three batches (one batch from each animal) of 120 serial 0.2-μm-thick sections. On the 60th section of each series we located a type 2 pneumocyte, cut through its nucleus, and then followed it in both directions through the serial sections, taking a photograph of the same type 2 pneumocyte in each section. In this way we have completely sectioned two type 2 pneumocytes and partially sectioned a third. In each section of each cell we have tabulated and measured the dimensions of any holes in the basal laminae. Through serial reconstruction it was possible to determine the numbers and sizes of holes in the basal laminae of the three type 2 pneumocytes.

Tissue sampling, pneumonia. A 2-mm slice was taken in a vertical, coronal plane from the region of the perfusion-fixed lungs of each pneumonia rabbit. Well-fixed pneumonia regions were identified by the colloidal carbon and by the blue coloration from the toluidine blue. One-millimeter cubes were cut from these black and blue slices and processed for transmission electron microscopy as follows. After washing, the tissue cubes were postfixed in buffered (0.1 *M* cacodylate at pH 7.4) osmium tetroxide for 1 hr at 25°C. After washing with distilled water these tissue cubes were dehydrated through ethanol and infiltrated with LR white (Polysciences, Warrington, PA). Five randomly selected blocks were thin-sectioned at 70–90 nm and stained with uranyl acetate and Sato's (1968) lead. These sections were used to observe the path taken by migrating neutrophils through the interstitium of the alveolar walls.

RESULTS

Endothelial Tight Junctions, Pericytes, and Fibroblasts

The lower magnification images that included the whole perimeter of the capillary were sufficient to permit determination of the loci of tight junctions on the thin wall, the thick wall, or the intersections of the thick and thin walls (Figs. 1a (low mag.) and 1b (high mag.)). In these micrographs we were also able to locate pericyte profiles around the perimeter of the capillaries and fibroblasts in the interstitium. The higher magnification images of each capillary were used to determine whether extensions of fibroblasts were present around the capillaries and whether or not these extensions contacted pericytes or endothelium.

From the 90 capillaries examined from the three rabbit lungs, the majority of the tight junctions were located at the corners where the thin walls intersected the thick walls of the capillaries (Fig. 2a). The majority of the remaining tight junctions were located on the thick walls of these capillaries (Fig. 2a). In the 90 capillaries examined from the three mice the majority of the tight junctions were located at the intersections of the thin walls with the thick walls or on the thick walls (Fig. 2b).

All pericyte profiles associated with the capillaries in both the rabbit and mouse lungs were located on the thick walls (Table 1). Approximately 40% of these pericyte profiles observed in each animal were adjacent to an endothelial tight junction (Table 1). Pericyte profiles were more numerous around the capillaries of rabbit lungs than around those of the mouse (Table 1).

Examination of each of the 180 thick wall/thin wall intersections of the 90 rabbit capillaries in the higher magnification images revealed that extensions of fibroblasts were present at 112 of these intersections. Ten of these fibroblast extensions were

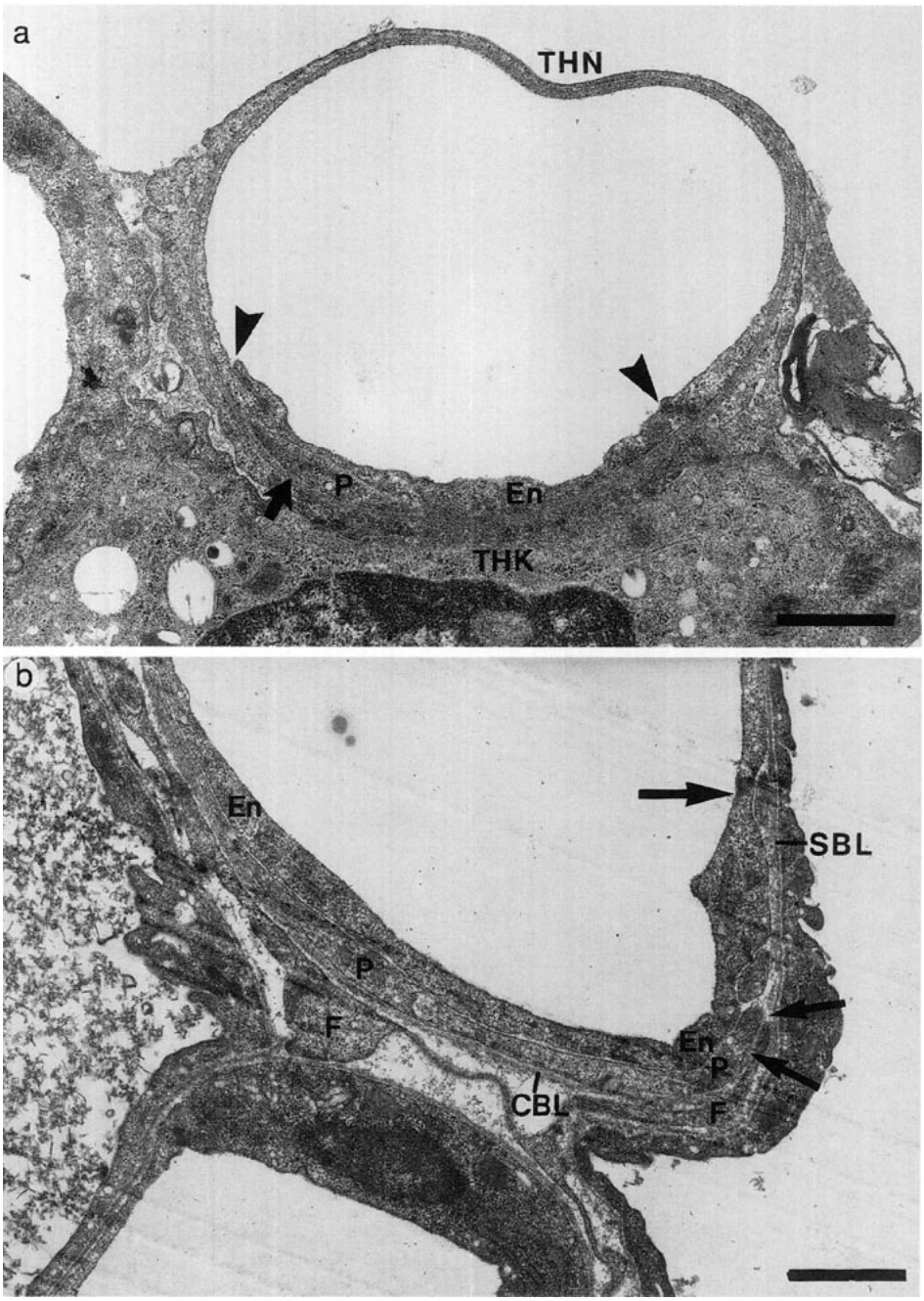

FIG. 1. (a) This is a cross section of an alveolar capillary photographed at 3000 to 6000×. Images like this were used to determine the presence and location of tight junctions and pericytes. The endothelial tight junctions (arrowheads) were located at the corners where thin (THN) and thick (THK) walls of the capillary intersect. A pericyte (P) lies adjacent to the endothelial cell (En) within the capillary basal lamina (arrow). Scale equals 1 μm. (b) The intersections of the thick and thin walls were photographed at 12,000 to 16,000×. At this magnification, holes (between small arrows) in the capillary basal lamina (CBL) were observed. At these holes, pericytes (P) were in contact with the endothelium (EN) and interstitial fibroblasts (F). The shared basal lamina of the capillary (SBL) begins here as well. This hole and pericyte/fibroblast cluster are in proximity to the endothelial tight junction (large arrow). Scale equals 1 μm.

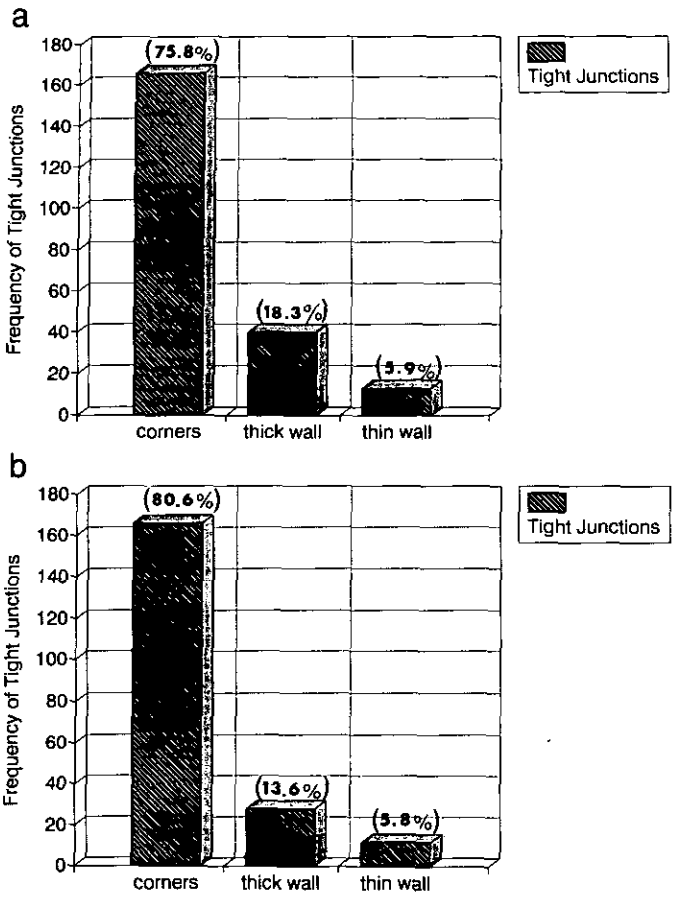

FIG. 2. Assessment of cross-sectioned alveolar capillaries of rabbits (a) and mice (b) show that the majority of tight junctions are located at the corners or on the thick walls. In the capillaries of rabbits, 94% of the tight junctions are located at the corners and on the thick walls, while only 6% of the tight junctions are located on the thin walls. The same is true for mice.

observed to penetrate the capillary basal lamina as in Fig. 1b. Twenty of the 180 intersections had no fibroblast extension present. A further 48 of the 180 intersections were sectioned so that fibroblast structure was obscured and therefore they were not used. Thus of the 180 thick wall/thin wall intersections 132 were usable and 9% of the 112 fibroblast extensions made close contacts with the endothelium in the rabbit lungs. In the mouse lungs 137 of the 180 intersections examined were sectioned so that fibroblast structure was clear. Ninety-one of these intersections had fibroblast extensions present and 5 of these made contact with endothelium through the capillary basal laminae. Thus in mouse lungs 5% of the fibroblast extensions were seen to contact the endothelium at these intersections.

Our observations of tight junctions, pericyte profiles, fibroblast extensions, and fibroblast contacts with endothelium or pericytes revealed that they are clustered at or near the intersections of the thick and thin walls of the capillaries. Between 75 (rabbits) and 80% (mice) of the endothelial tight junctions observed were located at

TABLE 1
Pericyte Profiles in Capillary Cross Section

	Animal 1	Animal 2	Animal 3
Rabbit			
Total no. on thick walls	33	36	15
No. adjacent to T.J. (% total)	12 (37)	12 (34)	8 (55)
Mouse			
Total no. on thick walls	21	6	4
No. adjacent to T.J. (% total)	7 (33)	2 (33)	2 (50)

Note. T.J., tight junction. All pericyte profiles were observed in the thick walls of alveolar capillaries and none were observed in the thin walls.

the intersections (Fig. 2). Approximately 40% of pericyte profiles in rabbits and mice were adjacent to endothelial tight junctions (Table 1). All of the remaining pericyte profiles were located on the thick walls of the capillaries (Table 1). Between 66 (mice) and 85% (rabbits) of intersections had extensions of fibroblasts present. Thus most tight junctions, pericyte profiles, and fibroblast extensions are located at the thick wall/thin wall intersections of the capillaries.

Endothelial Basal Lamina Holes

The 10 fibroblast extensions in the rabbit lungs and 5 in the mouse lungs that penetrated the capillary basal lamina to contact endothelium extended through holes in the basal laminae. All of these holes were located at the intersections of thick and thin walls of the capillaries where endothelial cells, pericytes, and interstitial fibroblasts made close contact (Fig. 1b). The serial sectioning of seven capillaries from three rabbit lungs included eight of these holes. The 20 serial sections of each capillary allowed us to reconstruct entire holes through the endothelial basal laminae. Their dimensions, determined by serial section reconstruction, showed that they were oval to slit-shaped and ranged in length from 0.43 to 1 μm (Table 2; Figs. 3a, 3b, and 3c).

Epithelial Basal Lamina Holes

In the sections used for assessing the loci of endothelial tight junctions and pericyte profiles, we consistently observed cytoplasmic extensions of the type 2 pneumocytes

TABLE 2
Holes in the Basal Lamina of Rabbit Alveolar Capillary

Rabbit	Hole length (μm)	Hole width (μm)
1	0.88	0.48
	1.00	0.24
2	0.67	0.32
	0.65	0.24
	0.84	0.16
3	0.43	0.24
	0.62	0.32
	0.80	0.32

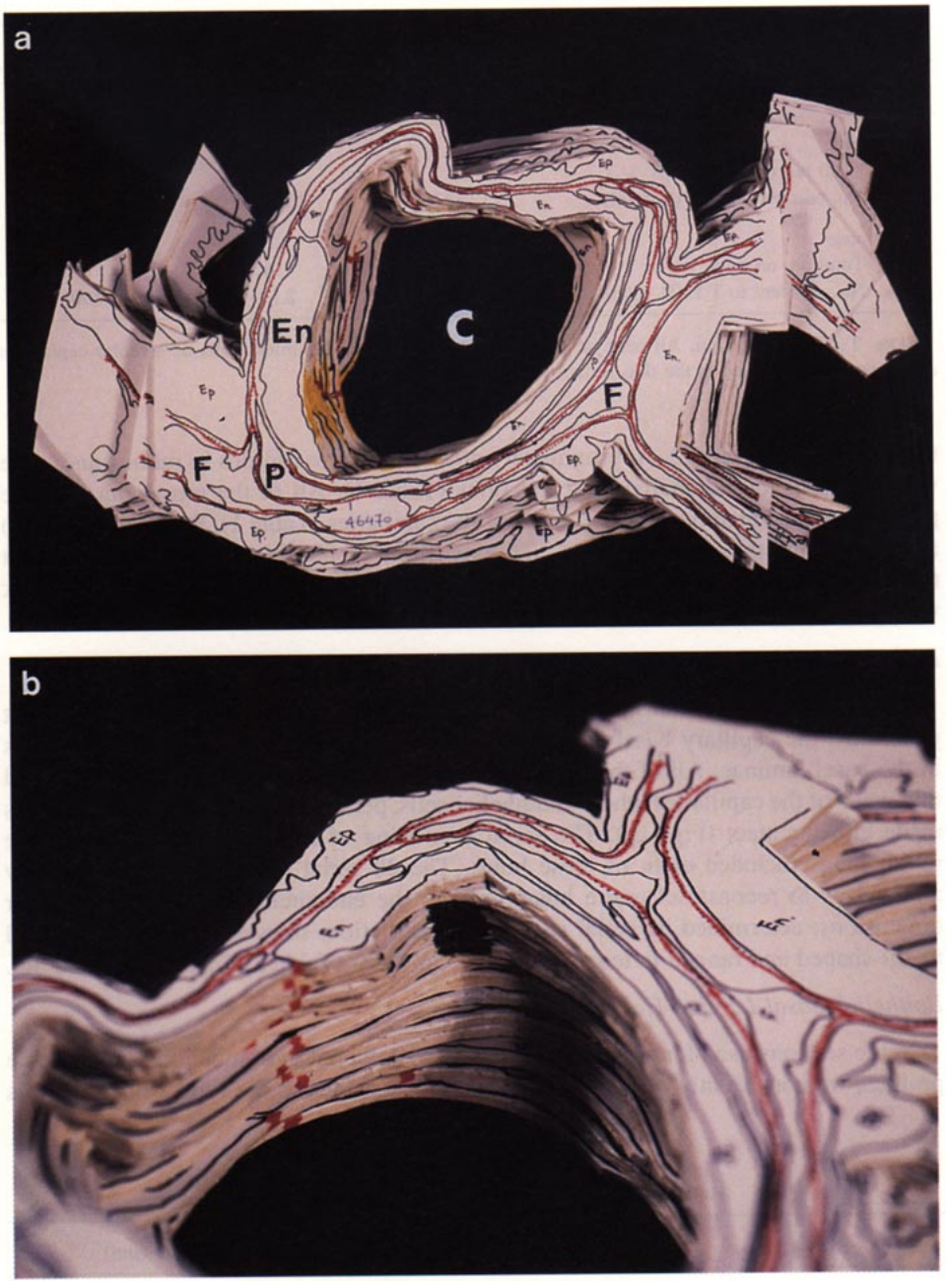

FIG. 3. Serial section reconstruction of a capillary in which two holes in the basal lamina are shown. (a) A 19-section serial reconstruction of an alveolar capillary (C). Note pericytes (P) in close contact with the endothelium (En) and within the capillary basal lamina (red line around the capillary). The absence of basal lamina between endothelium and pericytes constitutes a hole (areas like this are shown in the capillary lumen by yellow ink in c. Fibroblasts (F) also make contact with pericytes through holes in the basal laminae. *Two such holes are indicated with black ink on the capillary lumen in b and c.* (b) Note that the hole (black ink in capillary lumen) is located close to the endothelial tight junction (broken red line down capillary lumen) and at the intersection of the thick and thin walls. The approximate length of this hole is

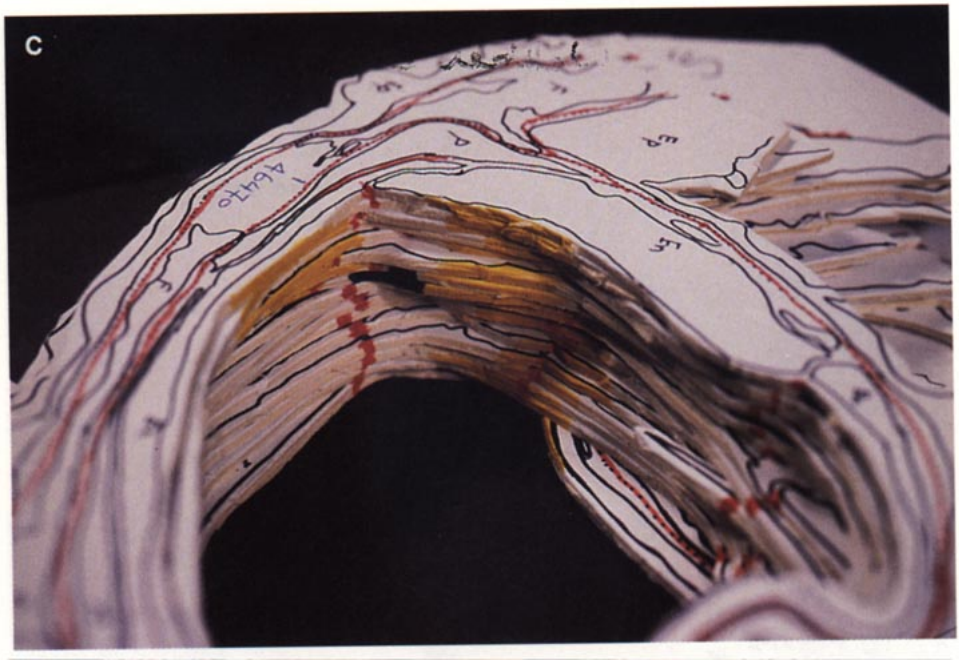

0.41 μm. (c) The gap associated with pericyte-endothelial contact is indicated by yellow ink in the lumen of the capillary. Note its proximity to the tight junction (broken red line in lumen of capillary) and to the location of the basal lamina hole (black spot in lumen).

through holes in their basal laminae that interdigitated with interstitial fibroblasts of the alveolar wall (Figs. 4a and 4b). In addition, hemidesmosome-like attachments were observed between the interstitial fibroblasts and the basal lamina of the type 2 pneumocyte in proximity to the interdigitations (Fig. 4a). One cytoplasmic extension of a fibroblast through a hole in the basal lamina of a type 2 pneumocyte was observed (Fig. 4b).

The observation of these connections between type 2 pneumocytes and fibroblasts was seen in all three serial-sectioned type 2 cells, suggesting that this is a common occurrence in rabbit lungs. The two type 2 pneumocytes that we completely serial sectioned required 55 and 60 0.2-μm thick sections. The third type 2 pneumocyte that was incompletely sectioned appeared in 36 sections. It is assumed that the 36 0.2-μm sections accounted for approximately $\frac{2}{3}$ of the cell. In the 55 sections that contained the first cell we observed nine holes in its basal lamina through which it made contact with three different fibroblasts. The second cell that required 60 serial sections had four holes in its basal lamina through which it made contact with at least two different fibroblasts. The range and means of the widths and depths of the basal lamina holes are given for each cell in Table 3. All of the type 2 pneumocytes serial sectioned had holes in their basal laminae. All of the holes observed spanned 1 to 5 0.2-μm thick serial sections.

Migrating Neutrophils

In the lungs of rabbits that had pneumonia of 2-hr duration, we observed migrating

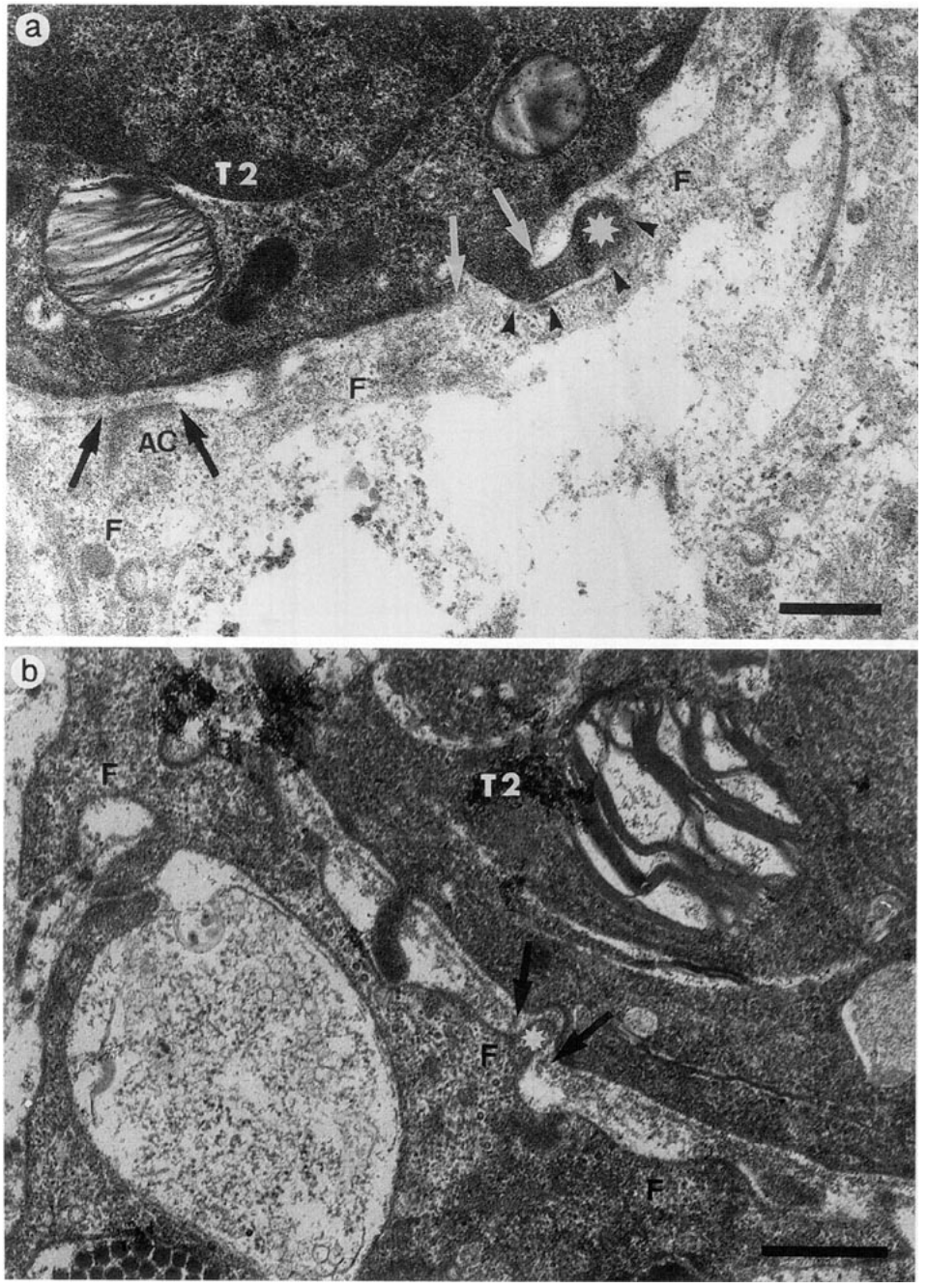

FIG. 4. (a) Cytoplasmic process of a type 2 pneumocyte (T2) that contacts an interstitial fibroblast (F). This process (white star) penetrates a hole in the basal lamina (between white arrows). The type 2 pneumocyte process is in close contact with the fibroblast (along arrowheads). A separate mechanical adherens contact (AC) is observed between the fibroblast and type 2 pneumocyte basal lamina (between black arrows). Scale equals 0.5 μm. (b) A cytoplasmic extension of a fibroblast (white star) that penetrates a hole in the basal lamina (between black arrows) of a type 2 pneumocyte (T2) and interdigitates with the

TABLE 3
Frequency and Dimensions of Holes in the Basal Lamina of Rabbit Type II Cells

	Rabbit 1	Rabbit 2	Rabbit 3
No of Holes/T-II cell	9	4	5
Width range (μm)	0.14–0.40	0.27–0.70	0.27–0.36
Width mean (μm)	0.29	0.43	0.34
Depth range (μm)	0.20–1.00	0.40–0.60	0.20–0.90
Depth mean (μm)	0.54	0.55	0.42

Note. T-II cell, Type II cell.

grating out of the capillaries and into the interstitium (Figs. 5a and 5b). Some of these neutrophils were in diapedesis across both the endothelial cells and endothelial basal lamina at the same time. Other neutrophils had already crossed the endothelium but were still in diapedesis across the basal lamina (Fig. 5a). These neutrophils also had to pass through a small hole in the basal lamina, as evidenced by their hourglass shape (Figs. 5a and 5b). Close examination of the isthmus of neutrophil cytoplasm between the interstitial pseudopod and the cell body remaining under the endothelium revealed the presence of numerous parallel microtubules (Fig. 5b). While the microtubules shown here are associated with the neutrophil granules, similar microtubule organization associated with the nucleus in the isthmus was observed in two other migrating cells. These migrating and interstitial neutrophils were observed to be adjacent to interstitial fibroblasts over some of their surface area (Fig. 5b).

We also observed neutrophils in various stages of migration from the interstitium into the airspace from below type 2 pneumocytes. Neutrophils were observed in contact with fibroblast/type 2 pneumocyte connections at holes in the basal lamina (Fig. 6a). In addition, we observed a neutrophil protruding into a hole in the type 2 cell basal lamina (Fig. 6b). Finally, we observed neutrophils migrating from the basal lateral space of type 2 pneumocytes and an adjacent type 1 pneumocyte into the airspace (Fig. 6a).

DISCUSSION

The results of this study establish that there are preexisting holes in the basal laminae of endothelial cells and pericytes at intersections of capillary thick and thin walls where endothelial cells, pericytes, and fibroblasts converge (Fig. 7). These holes have a slit-like shape and range from 0.43 to 1.0 μm in length and from 0.16 to 0.48 μm in width. Round holes that range in diameter from 0.14 to 0.7 μm were observed in the basal laminae of type 2 pneumocytes at points of contact with fibroblasts (Fig. 7). Deformed neutrophils were observed migrating through both of these holes during a streptococcal pneumonia in rabbits. These three observations support the hypothesis that inflammatory cells migrate through preexisting holes in the basal laminae of alveolar walls.

During inflammation in the lung, neutrophil migration begins with diapedesis across the endothelium of alveolar capillaries (Loosli and Baker, 1962; Shaw, 1980; Damiano

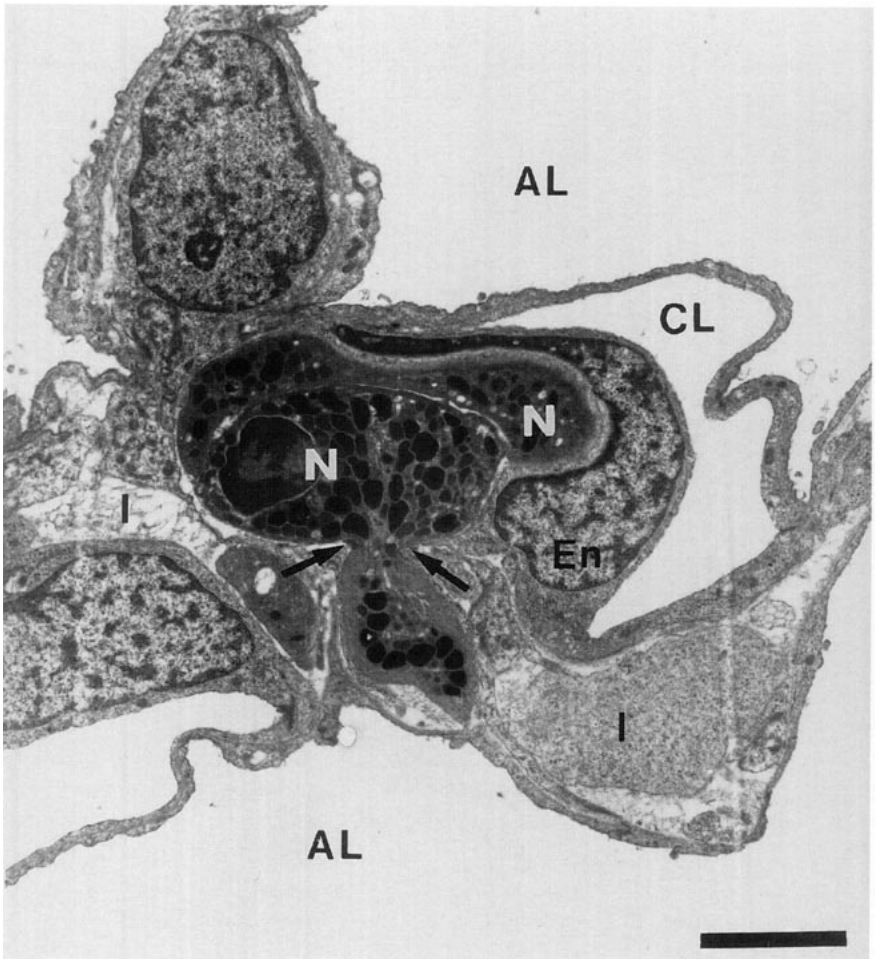

FIG. 5. (a) These neutrophils (N) have already emigrated from the capillary lumen (CL) across the endothelium (En). The hourglass-shaped neutrophil is passing through a hole (between arrows) in the capillary basal lamina into the interstitium (I). AL, alveolar lumen. Scale equals 2.5 μm. (b) Cytoplasmic isthmus of the neutrophil crossing the endothelial basal lamina (small arrowheads) into the interstitium in a. The pseudopod of the neutrophil is in close contact with fibroblasts (F) on both sides (small arrows). Three groups of parallel microtubules (large arrowheads) run through the isthmus. Scale equals 0.5 μm.

et al., 1980; Meyrick and Brigham, 1983; Walker *et al.*, 1991; Lien *et al.*, 1991). Previous observations of leukocyte migrations did not provide evidence of significant disruption of endothelial basal laminae (Majno and Palade, 1961; Marchesi and Gowans, 1964; Hurley, 1963; Hurley and Xeros, 1961; Shaw, 1980). In fact, Majno and Palade (1961) suggest that perhaps the basal lamina should be viewed as a sieve rather than an impenetrable barrier. However, they did not provide any specific information as to the nature of the basal lamina that would permit it to act as a sieve. Fisher (1982) has shown that the basal lamina of the rat lens behaves like a sieve to plasma proteins and that the parameters of this sieve are dynamic. Fisher demonstrated (*in vitro*) increased permeation of the lens basal lamina with increased pressure (Fisher,

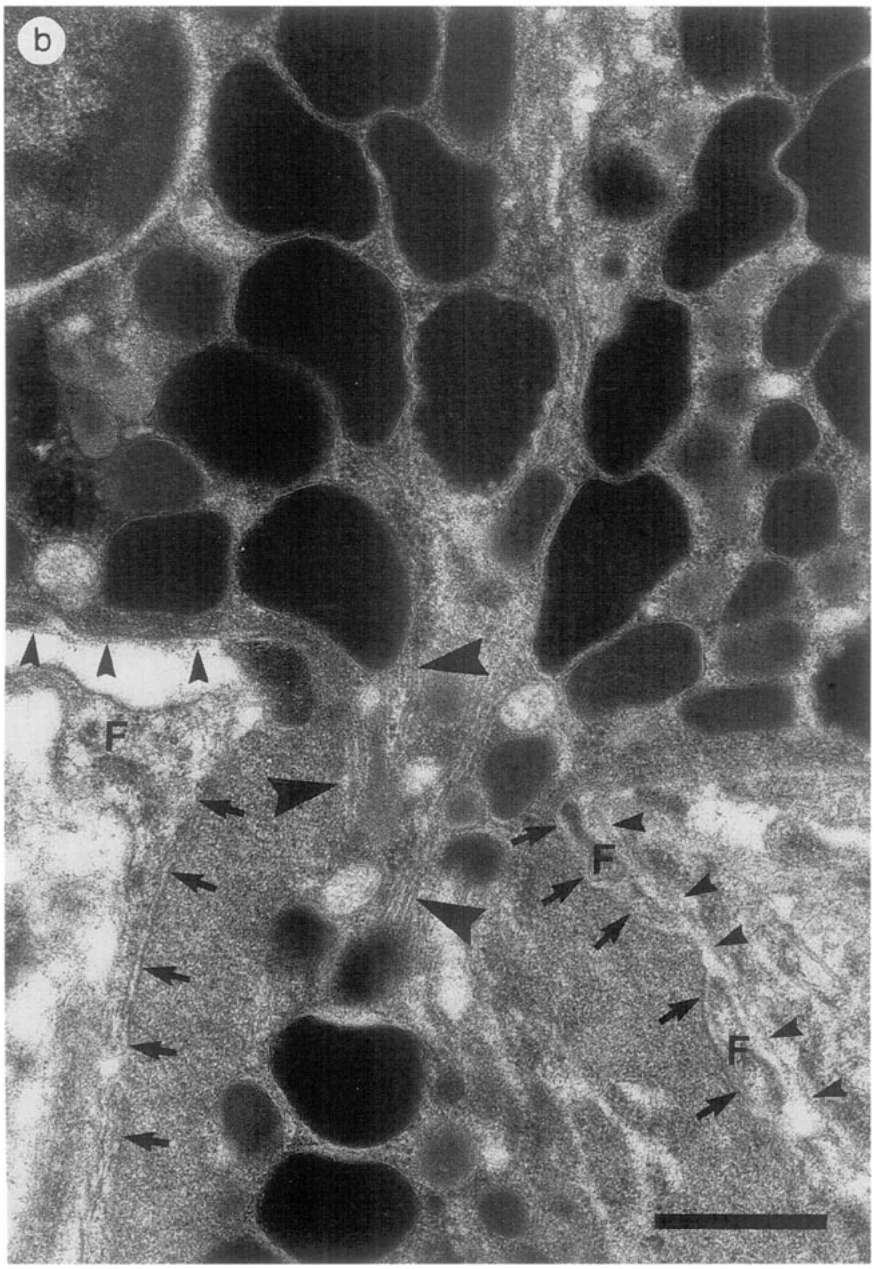

FIG. 5—*Continued*

1982). Although our *in vivo* observations from rabbit and mouse lung do not exactly support a sieve-like organization of the endothelial and epithelial basal laminae, they do suggest that neutrophils migrate through preexisting holes without damaging either basal lamina. Matzner *et al.* (1990) have shown that fibronectin associated with subendothelial basal lamina acts as a protective substrate that prevents unnecessary neutro-

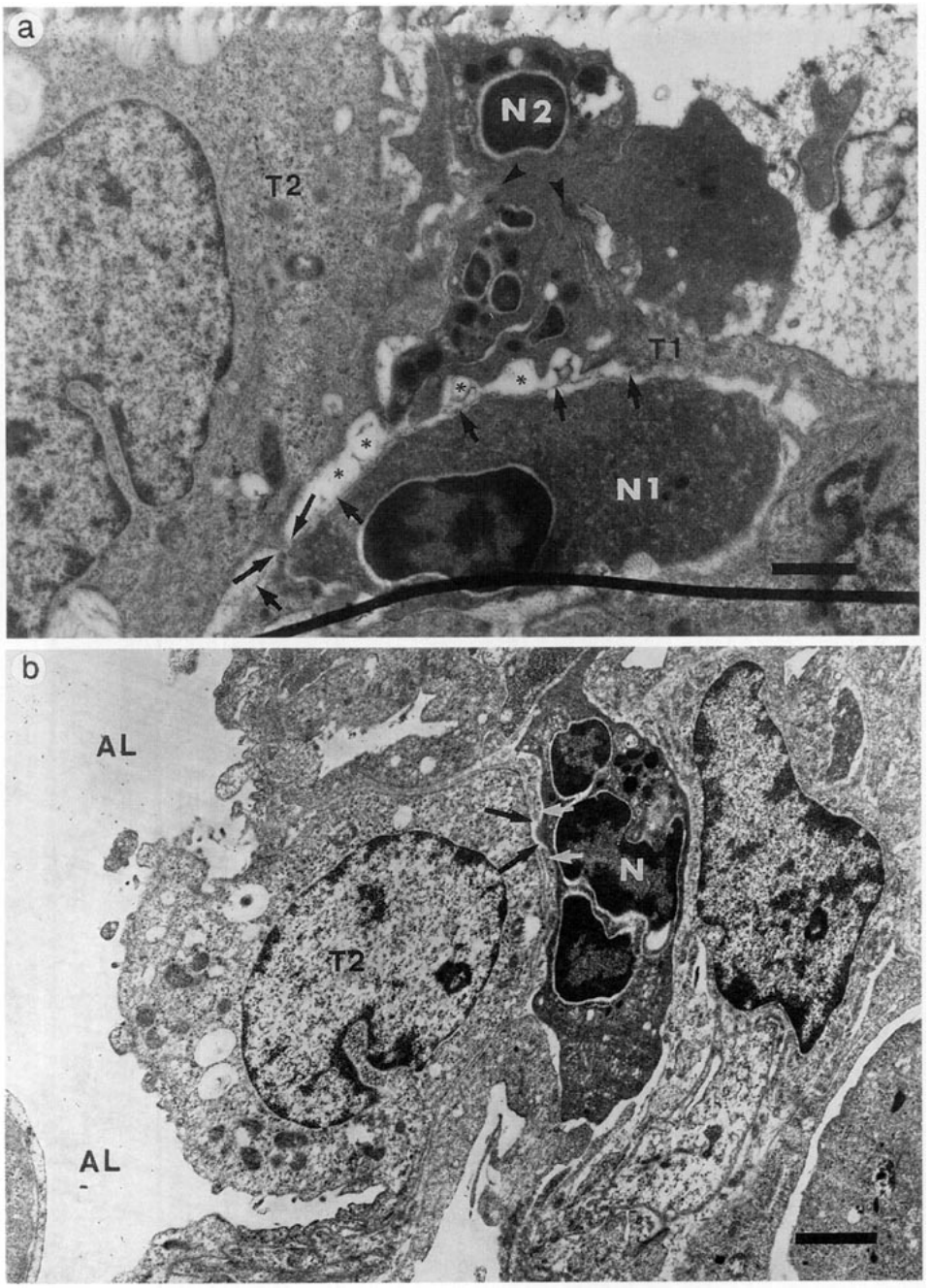

FIG. 6. (a) Two neutrophils migrating across the epithelium into the alveolar lumen of rabbit lung 2 hours after the instillation of *Streptococcus pneumoniae*. The lower neutrophil (N1) is still in the interstitium. It is in close contact with a fibroblast/type 2 cell connection (between long arrows). The upper neutrophil (N2) is in the process of diapedesis between the type 2 (T2) and type 1 pneumocyte (T1). Note the edges of the orifice the neutrophil is crossing (arrowheads) to enter the alveolar lumen. Finally, note the enlarged basal lateral space (asterisks) bounded by the type 2 cell and epithelial basal lamina (short arrows). Scale equals 1 μm. (b) A neutrophil (N) protruding into a hole (between black arrows) in the basal lamina below a type 2 pneumocyte (T2). Note that the profiles of fibroblast (white arrows) are displaced to either side and that the type 2 cell does not protrude into the interstitium. AL, alveolar lumen. Scale equals 2 μm.

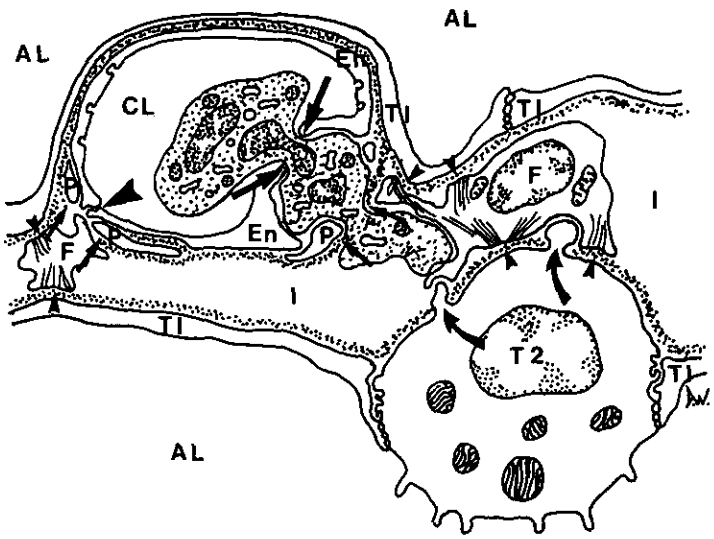

FIG. 7. A summary diagram of the pulmonary fibroblast connections with endothelial cells, pericytes, and type 2 cells that provide the holes in the basal laminae through which neutrophils migrate during pneumonia. This study demonstrates holes (between small arrows) in the endothelial basal lamina through which fibroblasts (F) contact pericytes (P) and endothelial (En) cells. These holes are located at the intersections of the thick and thin walls of the capillary in proximity to tight junctions (large arrowhead). Holes in the basal laminae of type 2 cells usually occur at points where projections of cytoplasm penetrate the basal lamina (curved arrows) and contact a fibroblast (F). In proximity to both types of holes, fibroblasts (F) are mechanically attached to the basal lamina of the epithelium (small arrowheads). This study demonstrates that diapedesis is a two-stage process. Neutrophils must first cross the endothelium (between large arrows) and then pass through the hole in the endothelial basal lamina (between small arrows). Observations suggest that neutrophils establish a close contact, if not adhesion, to the fibroblasts as they enter the interstitium. Neutrophils seem to displace the fibroblasts from the contact holes in both the endothelial and epithelial basal laminae in order to pass into the interstitium (I) and then into the airspace (AL).

phil activation and subsequent release of lysosomal enzymes during diapedesis. Borel *et al.* (1992) have shown that when neutrophils have previously been in contact with type IV collagen (a major constituent of alveolar capillary basal lamina; Gil and Martinez-Hernandez, 1984; Kefalides, 1979; Martinez-Hernandez and Amenta, 1983; Sage, 1982; Zibrak *et al.*, 1981) their activation by type I collagen (Monboisse, 1991), the δ1 (I) CB6 peptide, or bacterial peptide *N*-formyl-methionyl-leucyl-phenylalanine is inhibited. Huber and Weiss (1989) have shown that neutrophils pretreated with a potent serine protease inhibitor, diisopropylfluorophosphate, which drastically depressed the neutrophils' elastase and cathepsin G activity, successfully penetrated cultured subendothelial cell basal lamina. These studies (Matzner *et al.*, 1990; Borel *et al.*, 1992; Huber and Weiss, 1989) are consistent with the idea that migrating neutrophils do not release lysosomal enzymes in order to penetrate the basal laminae of the alveolar wall. Furthermore, the demonstration that the basal lamina is elastic (Fisher, 1982) suggests that neutrophils might mechanically enlarge the holes we have described as they migrate through them.

Sims and Westfall (1983) have shown that endothelial tight junctions are associated with pericyte profiles in a nonrandom fashion. They demonstrated that 39–55% of the pericyte profiles around alveolar capillaries are within 0.5 to 1 μm of endothelial

tight junctions. They also showed that profiles of pericytes are confined to the thick walls of the alveolar capillaries. In other tissues it has been shown that pericytes surround the capillaries and make numerous contacts with the endothelium (Rhodin, 1968; Sims, 1986, 1991a; Tilton, 1991). Others (Wakui *et al.*, 1989, 1990; Furusato *et al.*, 1990) have shown that numerous cytoplasmic interdigitations occur between the endothelium and the pericytes in immature capillaries of human granulation tissue. These observations make it clear that there are holes in the basal laminae of the endothelial cells through which they contact pericytes.

Endothelial cells also make contact with smooth muscle cells that lie in the interstitium below their basal laminae. Rhodin (1967) has shown that the endothelium of arterioles in the rabbit thigh produces foot-like processes which penetrate endothelial basal laminae and make contact with smooth muscle cells of the arterial wall. Michel (1982) has shown that pulmonary arterial endothelial cells penetrate the basal lamina to make gap junction contacts with underlying smooth muscle cells. The present study demonstrates that the endothelial tight junctions are preferentially located at the intersections of the thick and thin walls (Figs. 2a, 2b, and 7). This study also shows that pericyte contacts with the endothelium are confined to the thick side of the alveolar wall in both rabbit and mouse lungs (Table 1). Profiles of interstitial fibroblasts were also observed at the junction of the thick and thin wall where they made contact with the endothelium and pericytes through discontinuities in the basal lamina (Fig. 7). Since neutrophils were demonstrated in basal lamina discontinuities (Fig. 5a) at the same loci where we observed the holes occupied by fibroblasts in control rabbits, we conclude that the holes occupied by the fibroblasts are avenues through which neutrophils migrate into the extracellular compartment of the alveolar wall.

Damiano *et al.* (1980) have shown that during a lavage-induced inflammatory reaction in dog lung, neutrophils emerge into the airspace adjacent to the type 2 pneumocytes. To do this they must first cross the epithelial basal lamina. Adamson *et al.* (1990) and Vaccaro and Brody (1981) have both demonstrated discontinuities in the basal laminae of rat type 2 pneumocytes through which extensions of cytoplasm contact interstitial fibroblasts. Through morphometric analysis they estimated that these contacts occurred with a frequency of 0.5 and 0.7 per pneumocyte, respectively. Our observations confirm the presence of these holes in the lungs of rabbits. Furthermore, serial sections of three rabbit type 2 pneumocytes reveal that not only does each cell have multiple holes (Table 3) but also each is connected to more than one fibroblast.

Many investigators have demonstrated contacts such as these between embryonic epithelium and underlying mesenchymal cells (Trelstad *et al.*, 1967; Mathan *et al.*, 1972; Bluemink *et al.*, 1976; Adamson and King, 1984; Adamson *et al.*, 1991; Tarin and Croft, 1970). These contacts have been implicated in the epithelial/mesenchymal communication that is necessary for the embryonic development of tissues (Borghese, 1950; Grobstein, 1953; Masters, 1976; Goldin and Wessells, 1979; Sawyer and Fallon, 1983; Sanders, 1988). Normal tissue development does not appear to be possible without the presence of both epithelial and mesenchymal elements (Dameron, 1961; Golosow and Grobstein, 1962; Adamson *et al.*, 1991). It has been shown that, as tissue organization is established during lung development, the numbers of such contacts and their holes decline (Mathan *et al.*, 1972). These contacts between epithelium and interstitial cells, which are made possible by the presence of basal lamina discontinuities, play an important role in the organization of normal lung structure and function.

These fibroblast contacts with both endothelium and epithelium are not likely to play a mechanical role. Indeed, separate adherens-like junctions occur between fibroblasts and the basal laminae of type 1 and type 2 epithelial cells. Fibroblasts also make adherens-like contacts with the basal laminae of type 1 pneumocytes at the intersections of the thick and thin walls of the cross-sectioned capillaries (Figs. 1b and 7). They also make mechanical adherens-like contacts in immediate proximity to the holes in the type 2 cell basal lamina (Figs. 4a and 7). These mechanical contacts are distinguishable from those crossing the basal lamina by virtue of the bundles of microfilaments that terminate there. These mechanical contacts have been described by Kapanci (Kapanci *et al.*, 1974, 1979) and more recently by Sims (1991b). We suggest that neutrophils displace the nonmechanical contacts of the fibroblasts from the basal lamina discontinuities and then use these discontinuities as holes through which to migrate.

Although the diameter of the holes described in this paper are small, serial section data on a neutrophil in diapedesis across the endothelium showed that the neutrophils can migrate through a gap only 1 μm in diameter.

The presence of preexisting holes in the basal laminae of endothelium and epithelium at specific loci under endothelial tight junctions and epithelial type 2 cells supports the hypothesis that neutrophils can migrate from capillaries to the airspace without damaging alveolar wall basal laminae.

We suggest that migrating neutrophils displace the pericytes and fibroblasts from the basal lamina (Fig. 7) and pass through the existing hole which allowed these cells to make contact with the endothelium.

We postulate that neutrophils then find their way to the type 2 cells by crawling along fibroblasts in the interstitial space to the holes in the basal lamina through which the fibroblasts contact the type 2 pneumocytes (Fig. 7). This is supported by our observation that neutrophils entering (Fig. 5b) and leaving (Figs. 6a and 6b) the interstitium are in close contact with fibroblasts. By displacing the fibroblasts and type 2 cell extensions from these holes, the neutrophil is able to crawl into the basal lateral space of the type 2 cells from which it can then emerge onto the alveolar surface adjacent to the type 2 pneumocytes.

ACKNOWLEDGMENTS

The authors thank Professor James C. Hogg for reading this manuscript. We also thank Mr. Dean English for his assistance with surgery and Mr. Stuart Greene for his assistance with the photography for this manuscript. This work was supported in part by a grant from the B. C. Heart and Stroke Foundation and currently by MRC Grant 5-91232. The First Author is supported by the BC Lung Association and A. Behzad was supported by a summer studentship awarded by the Faculty of Medicine at UBC.

REFERENCES

Adamson, I. Y. R., and King, G. M. (1984). Sex differences in development of fetal rat lung: Quantitative morphology of epithelial mesenchymal interactions. *Lab. Invest.* **50,** 461–468.

Adamson, I. Y. R., Hedgecock, C., and Bowden, D. H. (1990). Epithelial cell–fibroblast interactions in lung injury and repair. *Am. J. Pathol.* **137,** 385–392.

Adamson, I. Y. R., Young, L., and King, G. M. (1991). Reciprocal epithelial: Fibroblast interactions in the control of fetal and adult rat lung cells in culture. *Exp. Lung Res.* **17,** 821–835.

Bluemink, J. G., Von Maurik, P., and Lawson, K. A. (1976). Intimate cell contacts at the epithelial/mesenchymal interface in embryonic mouse lung. *J. Ultrastruct. Res.* **55,** 257–270.

Borel, J. P., Bellon, G., Garnotel, R., and Monboisse, J. C. (1992). Adhesion and activation of human neutrophils on basement membrane molecules. *Kidney Int.* **43,** 26–29.

Borghese, E. (1950). Explanation experiments on the influence of the connective tissue capsule on the development of the epithelial part of the submandibular gland of *Mus musculus*. *J. Anat.* **84,** 303–318.

Brody, J. S., and Nancy, N. B. (1983). Proliferation of alveolar interstitial cells during postnatal lung growth, evidence for two distinct populations of pulmonary fibroblasts. *Am. Rev. Respir. Dis.* **127,** 763–770.

Cottrell, T. S., Levine, O. R., Senior, M. R., Wiener, J., Spiro, D., and Fishman, A. P. (1967). Electron microscopic alterations at the alveolar level in pulmonary edema. *Circ. Res.* **21,** 783–797.

Dameron, F. (1961). Influence de divers mesenchymes sur la differenciation de l'epithelium pulmonaire de l'embryon de poulet en culture in vitro. *C. Rend. Hebd. Acad. Sci. Paris* **252,** 3879–3881.

Damiano, V. V., Cohen, A., Tsang, A., Batra, G., and Petersen, R. (1980). A morphologic study of the influx of neutrophils into dog lung alveoli after lavage with sterile saline. *Am. J. Pathol.* **100,** 349–364.

Doerschuk, C. M., Winn, R. K., Coxson, H. O., and Harlan, J. M. (1990). CD18-dependent and -independent mechanisms of neutrophil emigration in the pulmonary and systemic microcirculation of rabbits. *J. Immunol.* **144,** 2327–2333.

Fisher, R. F. (1982). The water permeability of basement membrane under increasing pressure: Evidence for a new theory of permeability. *Proc. R. Soc. London* **B216,** 475–496.

Furusato, M., Wakui, S., Suzuki, M., Hori, M., Kano, Y., and Ushigome, S. (1990). Three dimensional ultrastructural distribution of cytoplasmic interdigitation between endothelium and pericyte of capillary in human granulation tissue by serial section reconstruction method. *J. Electron Microsc.* **39,** 86–91.

Gil, J., and Martinez-Hernandez, A. (1984). The connective tissue of the rat lung: Electron immunohistochemical studies. *J. Histochem. Cytochem.* **32,** 230–238.

Gil, J., and Weibel, E. R. (1969). Improvements in demonstration of lining layer of lung alveoli by electron microscopy. *Respir. Physiol.* **8,** 13–36.

Goldin, G. V., and Wessells, N. K. (1979). Mammalian lung development the possible role of cell proliferation in the formation of supernumerary tracheal buds and in branching morphogenesis. *J. Exp. Zool.* **208,** 337–346.

Golosow, N., and Grobstein, C. (1962). Epitheliomesenchymal interaction in pancreatic morphogenesis. *Dev. Biol.* **4,** 242–255.

Grobstein, C. (1953). Inductive epithelio–mesenchymal interaction in cultured organ rudiments of the mouse. *Science* **118,** 52–55.

Huber, A. R., and Weiss, S. J. (1989). Disruption of the subendothelial basement membrane during neutrophil diapedesis in an *in vitro* construct of a blood vessel wall. *J. Clin. Invest.* **83,** 1122–1136.

Hurley, J. V. (1963). An electron microscopic study of leucocytic emigration and vascular permeability in rat skin. *Aust. J. Exp. Biol.* **41,** 171–186.

Hurley, J. V., and Xeros, N. (1961). Electron microscopic observations on the emigration of leucocytes. *Aust. J. Exp. Biol.* **39,** 609–624.

Kapanci, Y., Assimacopoulos, A., Irle, C., Zwahlen, A., and Gabbaini, G. (1974). "Contractile interstitial cells" in pulmonary alveolar septa: A possible regulator of ventilation/perfusion ratio? Ultrastructural, immunofluorescence, and in vitro studies. *J. Cell Biol.* **60,** 375–392.

Kapanci, Y., Costabella, P., Mo, Cerutti, P., and Assimacopoulos, A. (1979). Distribution and function of cytoskeletal proteins in lung cells with particular reference to "contractile interstitial cells." *Methods Achiev. Exp. Pathol.* **9,** 147–168.

Kaplan, N. B., Grant, M. M., and Brody, J. S. (1985). The lipid interstitial cell of the pulmonary alveolus, age and species differences. *Am. Rev. Respir. Dis.* **132,** 1307–1312.

Kefalides, N. A. (1979). A collagen of unusual composition and a glycoprotein isolated from canine glomerular basement membrane. *Biochem. Biophys. Res. Commun.* **22,** 26–32.

Lien, D. C., Henson, P. M., Capen, R. L., Henson, J. E., Hanson, W. L., Wagner, W. W. Jr., and Worthen, G. S. (1991). Neutrophil kinetics in the pulmonary microcirculation during acute inflammation. *Lab. Invest.* **65,** 145–159.

Loosli, C. G., and Baker, R. P. (1962). Acute experimental pneumococcal (type 1) pneumonia in the mouse: The migration of leukocytes from the pulmonary capillaries into the alveolar space as revealed by the electron microscopy. *Trans. Am. Clin. Climatol. Assoc.* **74,** 15–28.

Low, F. (1961). The extracellular portion of the human blood-air barrier and its relation to tissue space. *Anat. Rec.* **139,** 105–111.

Majno, B., and Palade, G. E. (1961). Studies on inflammation. I. the effect of histamine and serotonin on vascular permeability: An electron microscopic study. *J. Cell Biol.* **11,** 571–605.

Marchesi, V. T., and Gowans, J. L. (1964). The migration of lymphocytes through the endothelium of venules in lymph nodes: An electron microscope study. *Proc. R. Soc. London B* **159,** 283–290.

Marko, M., Leith, A., and Parsons, D. (1988). Three-dimensional reconstruction of cells from serial sections and whole-cell mounts using multilevel contouring of stereo micrographs. *J. Electron Micros. Tech.* **9,** 395–411.

Martinez-Hernandez, A., and Amenta, P. S. (1983). The basement membrane in pathology. *Lab. Invest.* **48,** 656–677.

Masters, J. R. W. (1976). Epithelial–mesenchymal interaction during lung development: The effect of mesenchymal mass. *Dev. Biol.* **51,** 98–108.

Mathan, M., Hermos, J., and Trier, J. S. (1972). Structural features of the epithelio-mesenchymal interface of rat duodenal mucosa during development. *J. Cell Biol.* **52,** 577–588.

Matzner, Y., Vlodavsky, I., Michaeli, R. I., and Eldor, A. (1990). Selective inhibition of neutrophil activation by subendothelial extracellular matrix: Possible role in protection of the vessel wall during diapedesis. *Exp. Cell Res.* **189,** 233–240.

Meyrick, B., and Brigham, K. (1983). Acute effects of Escherichia coli endotoxin on the pulmonary microcirculation of anesthetized sheep. *Lab. Invest.* **48,** 458–470.

Michel, R. P. (1982). Arteries and veins of the normal dog lung: Qualitative and quantitative structural differences. *Am. J. Anat.* **164,** 227–241.

Monboisse, J. C., Garnotel, R., Randoux, A., Dufer, J., and Borel, J. P. (1991). Adhesion of human neutrophils to and activation by type I collagen involving a $\beta 2$ integrin. *Compt. Rend. Sean. de la soc. Biol. et ses Filiales.* **185,** 164–170.

Phipps, R. P. (1992). *Pulmonary Fibroblast Heterogeneity,* p. 336. CRC Press, Ann Arbor, MI.

Penny, D. P., Keng, P. C., Derdak, S., and Phipps, R. P. (1992). Morphologic and functional characteristics of subpopulations of murine lung fibroblasts grown *in vitro. Anat. Rec.* **232,** 432–443.

Rhodin, J. A. G. (1967). The ultrastructure of mammalian arterioles and precapillary sphincters. *J. Ultrastruct. Res.* **18,** 181–223.

Rhodin, J. A. G. (1968). Ultrastructure of mammalian venous capillaries, venules and small collecting veins. *J. Ultrastruct. Res.* **25,** 452–500.

Ryan, S. F., with assistance of Ciannella, A., and Dumais, C. (1969). The structure of the interalveolar septum of the mammalian lung. *Anat. Rec.* **165,** 467–484.

Sage, H. (1982). Collagens of basement membranes (Review) *J. Invest. Dermatol.* **79,** 51s–59s.

Sanders, E. J. (1983). Recent progress towards understanding the roles of the basement membrane in development. *Can. J. Biochem. Cell Biol.* **61,** 949–956.

Sanders, E. J. (1988). The roles of epithelial–mesenchymal cell interactions in developmental processes. *Biochem. Cell Biol.* **66,** 530–540.

Sannes, P. L. (1984). Differences in basement membrane-associated microdomains of type I and type II pneumocytes in the rat and rabbit lung. *J. Histochem. Cytochem.* **32,** 827–833.

Sato, T. (1968). Modified method for lead staining of thin sections. *J. Electron Micros.* **17,** 158–159.

Sawyer, R. H., and Fallon, J. F. (Eds). (1983). *Epithelial–Mesenchymal Interactions in Development,* pp. 3–25. Praeger, New York.

Shaw, J. O. (1980). Leukocytes in chemotactic-fragment-induced lung inflammation. *Am. J. Pathol.* **101,** 283–302.

Sims, D. E. (1986). The pericyte: A review. *Tissue Cell* **18,** 153–174.

Sims, D. E. (1991a). Recent advances in pericyte biology, implications for health and disease. *Can. J. Cardiol.* **7,** 431–443.

Sims, D. E. (1991b). Orientation of adhering junctions between bovine pulmonary fibroblasts. *Acta Anat.* **140,** 145–249.

Sims, D. E., and Westfall, J. A. (1983). Analysis of relationships between pericytes and gas exchange capillaries in neonatal and mature bovine lungs. *Microvasc. Res.* **25,** 333–342.

Tarin, D., and Croft, C. B. (1970). Ultrastructural studies of wound healing in mouse skin. II. Dermo–epidermal interrelationships. *J. Anat.* **106,** 79–91.

Tilton, R. G. (1991). Capillary pericytes. Perspect. *Future Trends Electron Micros. Tech.* **19,** 327–344.

Trelstad, R. L., Hay, E. D., and Revel, J-P. (1967). Cell contact during early morphogenesis in the chick embryo. *Dev. Biol.* **16,** 78–106.

Vaccaro, C. A., and Brody, J. S. (1981). Structural features of alveolar wall basement membrane in the adult rat lung. *J. Cell Biol.* **91,** 427–437.

Wakui, S., Fursato, M., Hasumura, M., Kano, Y., and Ushigome, S. (1989). Two and three dimensional ultrastructure of endothelium and pericyte interdigitation in capillary of human granulation tissue. *J. Electron Micros.* **38,** 136–142.

Wakui, S., Furusato, M., Tanaka, M., Allsbrook, Jr., W. C., Kano, Y., and Ushigome, S. (1990). Endothelium and pericyte interdigitation: Pathway for epidermal growth factor? *Microvasc. Res.* **40,** 285–291.

Walker, D. C., Chu, F., and Mackenzie, A. (1991). Pathway of leukocyte emigration from the pulmonary vasculature during pneumonia in rabbits. *Am. Rev. Respir. Dis.* **143,** A541.

Walker, D. C., Mackenzie, A., and Hosford, S. (1994). The structure of the tricellular region of endothelial tight junctions of pulmonary capillaries analyzed by freeze-fracture. *Microvasc. Res.* **48,** 259–281.

Wang, N. S., and Ying, W. L. (1977). A scanning electron microscopic study of alkali-digested human and rabbit alveoli. *Am. Rev. Respir. Dis.* **115,** 449–460.

Zibrak, J. D., Brody, J. S., Vaccaro, C., and Farris, B. (1981). Isolation and characterization of alveolar wall basement membranes purified with human skin collagenase. *Am. Rev. Respir. Dis.* **123,** A230.